



UNIVERSITÀ
DEGLI STUDI
FIRENZE

FLORE

Repository istituzionale dell'Università degli Studi di Firenze

Eye gaze patterns in emotional pictures

Questa è la Versione finale referata (Post print/Accepted manuscript) della seguente pubblicazione:

Original Citation:

Eye gaze patterns in emotional pictures / A. Lanatà; G. Valenza; Scilingo E.P.. - In: JOURNAL OF AMBIENT INTELLIGENCE AND HUMANIZED COMPUTING. - ISSN 1868-5137. - ELETTRONICO. - 4:(2013), pp. 705-715. [10.1007/s12652-012-0147-6]

Availability:

This version is available at: 2158/1192173 since: 2021-06-11T13:21:23Z

Published version:

DOI: 10.1007/s12652-012-0147-6

Terms of use:

Open Access

La pubblicazione è resa disponibile sotto le norme e i termini della licenza di deposito, secondo quanto stabilito dalla Policy per l'accesso aperto dell'Università degli Studi di Firenze (<https://www.sba.unifi.it/upload/policy-oa-2016-1.pdf>)

Publisher copyright claim:

(Article begins on next page)

Eye gaze patterns in emotional pictures

Antonio Lanatà · Gaetano Valenza ·
Enzo Pasquale Scilingo

Received: 30 September 2011 / Accepted: 29 February 2012 / Published online: 19 July 2012
© Springer-Verlag 2012

Abstract This paper reports on a preliminary study aiming at investigating the eye gaze pattern and pupil size variation to discriminate emotional states induced by looking at pictures having different arousal content. A wearable and wireless eye gaze tracking system, herein-after called HATCAM, which was able to robustly detect eye tracking and pupil area was used. A group of ten volunteers was presented with a set of neutral and arousal pictures extracted from the International Affective Picture System according to an ad-hoc experimental protocol. A set of features was extracted from eye gaze patterns and pupil size variations and used to classify the two classes of pictures. Although preliminary, results are very promising for affective computing applications.

Keywords Eye gaze tracking · Wearable systems · Affective computing · Emotions · Pattern recognition

1 Introduction

Emotions are psychological conditions that affect several human behaviors, relations, process and results of actions. They are present in all mental processes, and any human activity manifestation is accompanied by emotional experiences. Many works have shown that emotional processing can have primacy over cognition (Zajonc 1984). The famous naturalist Darwin stated that emotions emerged during the course of evolution as the means by which living

creatures determine the significance of certain conditions to meet their urgent needs (Darwin et al. 2002). Other works have shown how emotion regulation is an essential feature of the mental health. In particular, they highlighted how emotion and its regulation have an important role in various aspects of normal functioning. For example, emotions become dysregulated in major depressive episodes, and some theoretical views of depression are based on emotion changes which have implications in assessment, treatment, and prevention of the pathology (Gross and Muñoz 1995). Moreover, it has been shown that there exists strong relationship between emotion and anxiety (Lazarus and Averill 1972) as well as brain damages of emotional processing areas and decision-making process (Damasio 2000). In this viewpoint, the importance of having an automatic emotion recognition system becomes clear, which could be profitably used in several domains such as human behavior understanding, mental health investigation or social relations interpretation. Latest works on emotion recognition are based on the study of physiological correlates of the autonomic nervous system (ANS), e.g., heart rate variability, electrodermal activity (Picard 2000). The associations of emotions and physiological reactions controlled by the ANS are complex, but anger, for example, has been associated to a higher heart rate than happiness, and on the other hand, anger has been associated to higher finger temperature than fear (Ekman et al. 1983; Levenson 1992). In this work we aim at investigating the relationship between emotions and information coming from the eyes, i.e. pupil size variation and eye gaze pattern. It is known that pupil dilations and constrictions are governed by the ANS (Andreassi 2006). This work is a preliminary study on how eye tracking pattern and pupil area variation relate to emotional stimulation using images from the International Affective Picture System (IAPS). In other words, we want

A. Lanatà (✉) · G. Valenza · E. P. Scilingo
Department of Information Engineering,
Faculty of Engineering, Interdepartmental Research Centre
“E.Piaggio”, University of Pisa, Pisa, Italy
e-mail: a.lanata@centropiaggio.unipi.it

to explore the relationship between eye information and emotional image categories. More specifically, by using a head-mounted eye tracking system (named HATCAM) we acquired pupil variation together with eye gaze trajectory and time of fixation as well during the exposition of subjects to affective images having different levels of arousal. No familiar pictures were used and luminance was normalized in order to keep it constant. A specific set of features extracted from pupil size variation, eye gaze pattern and time of fixation was used as input to different classifiers in order to distinguish the neutral from arousal levels.

2 Background

In the literature several works can be found reporting emotional studies relating visual stimuli to eye gaze patterns. Some of them argued that when experiencing emotional events most of the attention is devoted to the emotional information rather than to detail information (Christianson et al. 1991; Bradley et al. 2003). Recently, some works reported on how eye tracking information can be related to selective attention to emotional pictorial stimuli (Calvo and Lang 2004). They found out that preferential attention depends on the affective valence of visual stimuli, i.e. pleasant and unpleasant pictures. Nevertheless, attention can be influenced by other emotional characteristics of pictorial stimuli, such as arousal, as well as by nonemotional characteristics, such as picture luminance, complexity, familiarity, and filled area with details. Concerning information provided by the pupil, previous studies have suggested that pupil size variation is related to both cognitive and affective information processing (Partala and Surakka 2003). More specifically, Beatty and Lucero-Wagoner (2000) pointed out that during cognitive tasks such as recalling something from memory, paying close attention, parsing a complicated sentence, or thinking hard, the pupils dilate and return to previous size within a few seconds of completing the mental work. Commonly, it is referred to as Task-Evoked Pupillary Response (TEPR), and even though the dilation was small, it resulted an involuntary act and reliably associated to a set of cognitive processes defined as cognitive load. As a matter of fact, previous works on affective elicitation and pupil size variation have been somewhat controversial. Dated research activity of Loewenfeld (1966) studied the effects of various sensory and psychological stimuli to pupil size variation and argued that none of them caused pupil constriction except for increased light intensity. On the contrary, Hess (1972) found out that there would be a continuum ranging from extreme dilation due to interesting or pleasing stimuli to extreme constriction due to unpleasant or distasteful

content. Almost in the same years, Janisse (1974) contradicted this bi-directional view arguing that there is no pupil constriction in response to negative stimuli, or it can be limited to a few individuals and a small range of stimuli. He proposed that pupil size should be linearly related to the stimulation intensity. From this point of view, pupil size variation seems to be sensitive to the valence scale, resulting largest at the negative and positive ends of the continuum and smallest at the center, that would represent neutral affect. The latest work of Partala and Surakka (2003) reported a study concerning on pupil size variation during and after auditory emotional stimulation. Their results showed that pupil size was significantly larger after both negative and positive than neutral stimulation. These results suggested that the autonomic nervous system is sensitive to systematically chosen highly arousing emotional stimulation. It is reasonable that the above contradictory results and theories may be due to the variety of stimuli used. Mostly, they have been limited sets of pictures varying in content, and they have suffered from methodological problems with color, luminance, and contrast (Hess and Petrovich 1987). Clearly, controlled stimulus set is a fundamental precondition requirement for a systematic study of the effects of emotions to pupil size variation. Nowadays, eye-tracking technology development (e.g. ease of use, improved accuracy, and enhanced sampling rate), offers the possibility for an unobtrusive monitoring of emotion-related reactions because no sensors need to be attached to the user. In order to be able to evaluate the possibilities of using pupil size measurement as well as pupil tracking for detecting emotional responses, we need to understand how emotions and eye features relate to each other. Eye movements can provide detailed estimates of what information an individual is considering rather quickly (in less than 200 ms). Eye tracking is becoming an increasing popular measure of cognitive and affective information processing (Lohse and Johnson 2002). By gathering data on the location and duration of eye fixations, many inferences about the cognition structure could be done. The use of eye tracking in estimating cognitive or affective states can be focused on two assumptions: the immediacy (people process information as it is seen) and the eye-mind (the eye remains fixated on an object while the object is being processed). A variety of eye-tracking methods exist. In terms of the data collected from the eye, two popular methods are mostly used. The first implies shining a light on the eye and detecting corneal reflection, the latter implies simply taking visual images of the eye and then locating the dark pupil area. Generally, the choice of the best method depends upon the external lighting conditions. To compute where a person is fixating, there are three popular methods. The first method simplifies the calculations by having fixed geometries by forcing the

person to hold still by biting on a bar or putting the head in a restraint, commonly these systems are referred to as remote eye trackers they have the advantage of using high sampling frequency camera to acquire the movements of the eye. The most used systems based on this methodology are *EyeLink 1000* Ltd. (2010), *ASL Model 504 L*. (2009), *Tobii 1750* Technology (2011) and *SMI RED I*. (2011). In the second method the person wears a head sensor that tracks the head orientation and location in three dimensions and then combines this information with eye-direction, this technique is the less used. The third method, used in our experiments, places the eye-tracking apparatus on the person head along with a camera so that a visual image is captured showing what the person is currently looking at, commonly these system are referred to as head mounted eye trackers, examples of systems using this technique are: *EyeLink II*, *ASL H6*, *Tobii Glasses system*, *Open-Eyes* Li et al. (2006), *ISCAN Inc.* (2007) and *iVIEW HED*, and our *HATCAM*. The advantage in using a head mounted eye tracker is of making the user free to move during the stimulation. The *HATCAM* used in our experiments is cheap, lightweight, wireless therefore based on a real-time detection of the eye gaze point and pupil size; it exploits brightness normalization algorithms and does not use infrared illuminators. Brightness normalization allows us to use the system in different light conditions, e.g. darkness or sunlight. The absence of infrared illuminators offers several advantages. Indeed, even though low-power infrared LEDs are, generally, employed to avoid injuries, the use of infrared illuminator systems, especially for high-sensitive subjects (e.g. children), can produce reddening and lachrymation. Furthermore, in subjects with eye glasses the lens disturb the infrared light thus showing very weak pupils. Finally, a large variation of bright light sources can produce a diminished image of the pupil or even its disappearance. These limitations in eye tracking methods using infrared illuminators impose stable lighting conditions, and therefore a restriction of the fields of application.

A crucial issue is the methodology for eliciting different emotional states. In this view, several works, e.g. Lang et al. (1997), report a set of systematically studied affective image stimuli belonging to the International Affective Picture System (IAPS). These stimuli have been studied using the Self-Assessment Manikin, which is a method to study differences in affective experiences using nine-point bipolar rating scales. In these works, subjects look at the stimuli and ranked them on three bipolar dimensions: emotional valence, arousal, and dominance. However, valence and arousal are the most frequently used dimensions to capture the nature of emotional information. The valence dimension varies from negative to positive emotional experience, and the arousal dimension varies from

calm to highly excited. This kind of elicitation is used in our experiments.

3 HATCAM: wearable EGT system

The system used in this experiment, *HATCAM*, is a wearable and wireless eye tracking system which can be tailored to both adults and children. It is comprised of only one lightweight camera which is able to capture, by means of a mirror, the eyes of the subject and the scene in front of him, simultaneously. The system configuration is shown in Fig. 1. The system is comprised of a wireless CMOS camera (CP294) having low weight (20 g), low size ($2 \times 2 \times 2$ cm), and an A/V transmitter. The camera has a resolution of 628×586 pixels with $F2.0$, $D45^\circ$ optic, and 25 frames per second (f.p.s.). The original lens of the camera was removed and substituted with a wide-angle-lens without IR filter. This operation allows enlarging the view angle and acquiring infrared components, which emphasize the contrast between pupil and iris. This system is able to capture simultaneously, without latency, the visual scene in front of the subject and the position of his eyes. This is achieved using a mirror (4×0.6 cm) placed on a shaft linked to the head (see Fig. 1). Tilt and shaft of the mirror and the camera orientation can be tailored to user forehead profile (see Fig. 1).

4 Experimental protocol

Ten subjects, nine males and one female, volunteered to participate in the experiment. All subjects did not suffer from mental pathologies. Six subjects had dark eyes and four had bright eyes. The average age was of 26.8 with a standard deviation of 1.5. The experiment was performed in a room with controlled illumination condition achieved by white neon lighting equally distributed over the room

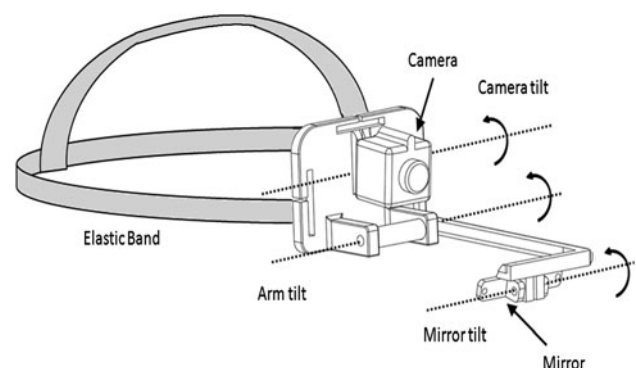


Fig. 1 HATCAM configuration

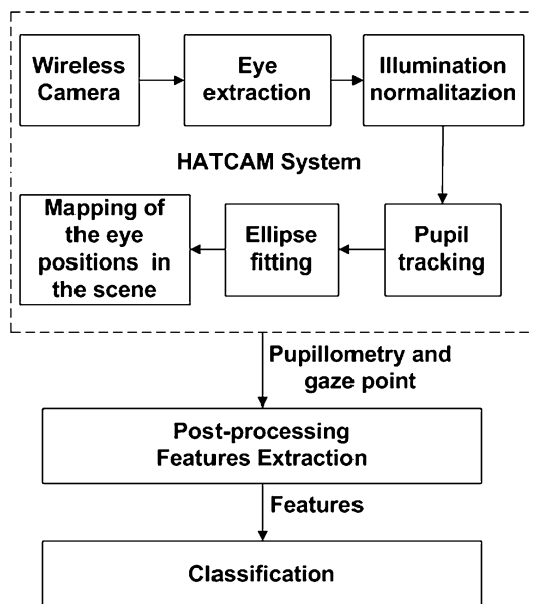


Fig. 2 Block diagram showing all the algorithmic stages of the processing of eyes and outside scene

with a power of 50 lumens. The HATCAM can work allowing the subjects wearing it to move freely their head, but in this specific experiment, in order to have a reliable and accurate measurement of the pupil size variation (which is more critical than eye gaze tracking) we decided to use a chin-support. Subjects were asked to sit on a comfortable chair 70 cm far from a screen. They were presented with a sequence of images, gathered from the IAPS database, while wearing headsets for acoustical insulation. The slideshow was comprised of 5 sessions of images N, A, N, A, N , where N was a session of 5 neutral images, and A were sets of 5 images having maximum level of arousal and the lowest valence, i.e. high negative affective impact. During the experiments all the subjects were asked to look at the picture which appeared on the screen for 10 s. Each trial lasted about 25 min. Each image was remapped in grey scale with constant histogram in order to provide images with a similar level of luminance.

5 Pupillometry and gaze point

This section deals with the processing techniques used to detect the center of the eye and how its movements were mapped into the image plane, i.e. the plane corresponding to image acquired by the camera. This technique is often referred to as Video OculoGraphy (VOG) and involves visible spectrum imaging. It is a passive approach that captures ambient light reflected by the eye. The lens inside the mounted camera was modified to acquire also the IR components from the natural light. Since the natural light

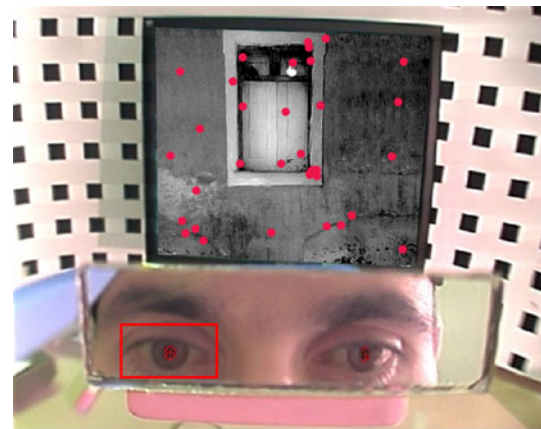


Fig. 3 Example of a single frame captured by the camera. The rectangular area marked up in red represents the ROI (color figure online)

spectrum comprises also the near-infrared region of the electromagnetic spectrum, the system kept the advantages of IR illumination of increasing the contrast between pupil and iris, and at same time preventing any possible injuries due to artificial IR illuminators, as no illuminators towards the eyes were used. Figure 2 shows the block diagram of the algorithmic process used to classify visual stimuli having different affective arousal content. The upper block implements the pupillometry and gaze point identification. The output was then processed to extract a specific set of features used for the classification. Specifically, the pupillometry and gaze point block was comprised of a sub-chain of blocks implementing the eye extraction algorithm, photometric normalization algorithm of illumination, pupil contour and mapping of the eye center into the image scene. Hereinafter we will describe briefly how eye and pictures were processed, but further details can be found in Armato et al. (2011). Figure 3 shows how the HATCAM is able to acquire simultaneously the eyes of the user and the scene in front of him using the mirror. Eye extraction procedure was constituted of visual inspection of the first video frame, in which a rectangular area including the eye was manually selected. This region is called Region Of Interest (ROI). Since the system mounted on the head, the ROI did not change throughout the experiment. In addition, only the red-image-component was converted in grey scale and used as input to the other processing blocks, as this component was specifically helpful in enhancing the contrast between pupil and background. as shown in grey scale and modified in terms of illumination normalization in order to reduce or eliminate some variations in the captured eyes due to different light conditions. In this work, we used the Discrete Cosine Transform (DCT) already proposed by Chen et al. (2006). This algorithm was already shown to be the suitable illumination normalization technique for

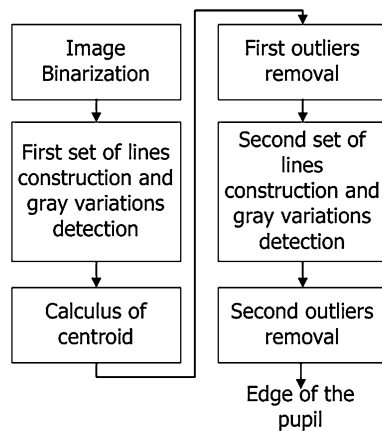


Fig. 4 Block diagram of the pupil tracking algorithm

realtime eye tracking processing in our previous work (Armato et al. 2011). This approach is based on the Retinex theory (from the words “retina” and “cortex”, suggesting that both eye and brain are involved in the processing) developed by Land and McCann (1971). This theory is based on the color constancy assumption which ensures that the perceived color of objects remains relatively constant under varying illumination conditions. Land and his colleagues assume that the stimulus is not the result of the light source and surface reflectivity only, but that the visual system processes the stimulus, integrating the spectral radiance and generating a ratio of integrated radiance of any region of the scene with that of the brightest region.

A specific pupil tracking algorithm was applied to extract the contour of the pupil exploiting the higher contrast of the pupil than the background due to the IR components of the natural light. Figure 4 shows the algorithm block diagram. The first block binarized the image by means of a threshold. After binarization, two sheafs of lines starting from the middle points of the vertical sides of the image, with an angular aperture of 30° , were drawn. As result of the binarization process, the image borders were expected to belong to the background, therefore the starting point of each line has a value of 255 in terms of grey level. Analogously, the pupil was expected to be placed roughly in the middle of the image (this is assured by an accurate manual selection of the ROI). When each line encounters, along its path, a dark pixel, this latter can be thought to belong to the contour of the pupil. Afterwards, the centroid of these points was calculated. After removing all the outliers, being these points very far from the centroid with respect to the large point density (pupil edge), a large-grain approximation of the contour was obtained. Next, a sheaf of lines started from the centroid with an angular aperture of 360° , and detected all discontinuities, but this time from black to white. Finally, outliers were again removed. The result of this algorithm was a set of points constituting the pupil edge (see Fig. 5). Afterwards, in order

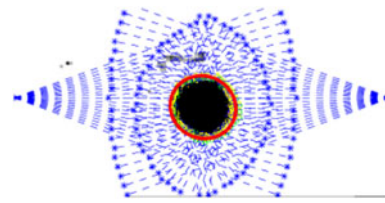


Fig. 5 Pupil tracking algorithm. Sheafs of lines are in blue; black points identify the eye including the outliers; yellow points highlight the pupil contour which is interpolated by the ellipse marked up in red (color figure online)

to construct the pupil contour and detect the center of the eye a specific ellipse fitting algorithm was implemented. Ellipse is considered as the best geometrical figure approximating the eye contour. In the literature, several ellipse fitting algorithms can be found and usually they can be divided into two broad techniques: the clustering/voting (CV) and the least square (LS) techniques. The first one uses two main approaches such as RANSAC and Hough Transform which are extremely robust but they are time-demanding or excessively resource consuming for real time machine vision (Forsyth and Ponce 2002; Bennett et al. 2002). In this work, we used the LS technique, i.e. a custom algorithm based on the algebraic distance with a quadratic constraint (Fitzgibbon et al. 2002), where a gaussian noise is added for the algorithm stabilization, (Maini 2005), to calculate the center of the pupil (that coincides with the ellipse center), the axes as well as the eccentricity of the ellipse. After the eye center was identified, a dedicated mapping procedure associated it to the image plane of the scene, providing as result the gaze point.

5.1 Post-processing and feature extraction

Post-processing phase was applied to a set of features extracted from the analysis of the eye gaze pattern matrix as well as to features extracted from Recurrence Quantification Analysis (RQA). This technique is usually used for nonlinear data analysis applied to dynamical systems. More specifically, it quantifies the number and duration of recurrences of a dynamical system presented by its phase space trajectory. The idea of using the latter technique, which is completely new to this field, arose from the analogy between the recurrence matrix plots of RQA and the matrices of eye gaze patterns. The features extracted from eye gaze analysis provided information about pupil dilation, max fixation time, length of eye gaze path, and most visited area in the image. In addition we extracted a set of features typical of the Recurrence Quantification Analysis (RQA). More specifically, as described in the experimental protocol, each image of the sequence was watched by the subjects for a time interval of 10 s. As the camera acquired with 25 frames per second, we obtained a grand total of 250 frames for each image. Each image can be represented as a

matrix of 628×586 pixels. The gaze point was mapped into a pixel in each frame. We constructed, therefore, a matrix of 628 rows and 586 column where each element corresponding to the pixel coordinates of the gaze point is set to 1. In order to minimize errors due to eye blinking and to instrumentation noise, only the pixels retained for at least five consecutive frames (0.2 s) were set to 1. At the end of this part we obtained a set of matrices of ones and zeros, having the same dimensions of the images. If the element (i, j) of a matrix, associated to a specific image, is one, it means that the pixel (i, j) of that image was observed at least for 0.2 s. In the next sections each feature is explained in detail.

5.1.1 Recurrence quantification analysis

The RQA (Zbilut and Webber 1994) is an advanced technique of nonlinear data analysis which reveals all the times when the phase space trajectory of the dynamical system visits roughly the same area in the phase space. In this work, we used the matrices of the gaze pattern as recurrence plot matrices, disregarding the multiple recurrences of the same gaze point. Let GP be the Gaze Plot matrix. Let $L_{ij}(x, y)$ be the set of eye-gaze points from the frame i of the image j , where x and y are spatial coordinates. We applied the RQA to the set $G_m(x, y)$ defined as:

$$G_m(x, y) = \bigcup_i L_{ij}(x, y)$$

For each image the following features were calculated: Recurrence Rate (*RR*) is the percentage of gaze points in an GP, it can be considered as the density of gaze points into an image:

$$RR = \frac{1}{N^2} \sum_{x,y=1}^N G_m(x, y)$$

where N is the number of points forming the image. Determinism (*DET*) is the percentage of gaze points which form diagonal lines:

$$DET = \frac{\sum_{l=l_{min}}^N lP(l)}{\sum_{i,j=1}^N R_{i,j}} \quad (1)$$

where $P(l)$ is the histogram of the lengths l of the diagonal lines. Trapping Time (*TT*) is the average length of the vertical lines:

$$TT = \frac{\sum_{v=v_{min}}^N vP(v)}{\sum_{v=v_{min}}^N P(v)} \quad (2)$$

Averaged diagonal line length (L) is the average length of the diagonal lines:

$$L = \frac{\sum_{l=l_{min}}^N lP(l)}{\sum_{l=l_{min}}^N P(l)} \quad (3)$$

Entropy (*ENTR*) is the Shannon entropy of the probability distribution of the diagonal line lengths $p(l)$:

$$ENTR = - \sum_{l=l_{min}}^N p(l) \ln p(l) \quad (4)$$

Longest diagonal line (L_{max}) The length of the longest diagonal line:

$$L_{max} = \max(\{l_i; i = 1, \dots, N_l\}) \quad (5)$$

where N_l is the number of diagonal lines in the gaze plot.

5.1.2 Fixation time

While watching each image, subject eye can be caught by specific details. We define as fixation time of each pixel, the absolute time during which the subject is dwelling on that pixel during the 10 s of presentation of each image. We obtain a statistical distribution of fixation times over the pixels, whose mode, which we define here as T_{max} , is used as feature. T_{max} is calculated for each image and each subject during both neutral and arousal elicitation as:

$$T_{max} = \text{Max}_{i=0}^N (t(p_i)) \quad (6)$$

where N is the number of points of gaze in the image, P_i is the i th point of gaze, $t(P_i)$ is the fixation time of the i th point of gaze, respectively.

5.1.3 Pupil area detection

The pupil was approximated as an ellipse whose area is calculated. To increase the robustness of the algorithm an averaged area of both eyes was considered:

$$A_p = \frac{\pi r_a^l r_b^l + \pi r_a^r r_b^r}{2} \quad (7)$$

where A_p is the pupil area, r_a^l and r_b^l are the ellipse semi-axes of the left eye, r_a^r and r_b^r are the ellipse semi-axes of the right eye.

5.1.4 Most visited area in the image

While looking at an image, there are areas more fixated than others. We define as Most Visited Area (MVA) in the image, the area of each image on which each subject lingered longer. Specifically, we defined an area of the image of $n \times n$ (where $n < N$) pixels, which was centered on the most watched pixel, and the MVA was calculated as the sum of the fixation times of all the pixels inside this area.

This feature was calculated for all images. Let $T(x, y)$ be the time of fixation of the pixel whose coordinates are x, y . Since $T_{max}(x_c, y_c)$ is the maximum time of fixation of the image and (x_c, y_c) are the coordinates of the most watched pixel. We calculated the MVA as:

$$MVA = \sum_{x,y=x_c-\frac{n}{2},y_c-\frac{n}{2}}^{x_c+\frac{n}{2},y_c+\frac{n}{2}} T(x, y)$$

where n is taken as forty pixels.

5.1.5 Length of the gaze path

The Length of the Gaze Path (LGP) of each image was calculated as the total length of the gaze path while the image was presented. We approximated the path between two consecutive points of gaze as a straight line, as two consecutive gaze points were obtained from two consecutive frames, i.e. in a time interval of 1/25 s. The distance between two points was calculated as Euclidean distance.

$$LGP = \sum_{x,y=1}^N \sqrt{(x_i - x_{i+1})^2 + (y_i - y_{i+1})^2} \tag{8}$$

5.2 Classification

The aim of this work was to classify two classes of images, labeled as neutral and arousal. Generally, the choice of one classifier rather than another depends on many factors, among which the type of particular distribution of the features considered into the analysis. The distribution can be gaussian or non-gaussian thus suggesting to use a parametric or non-parametric classifier, respectively. In this work the sets of extracted features exhibited non-parametric distributions, therefore non-parametric classifiers (Duda et al. 2001), i.e. Linear Discriminant Classifier (LDC), Quadratic Discriminant Classifier (QDC), Mixture Of Gaussian (MOG), k-Nearest Neighbor (k-NN), Kohonen Self Organizing Map (KSOM), Multilayer Perceptron (MLP), and Probabilistic Neural Network (PNN), were used. Best results have been achieved by the MultiLayer Perceptron (MLP) classifier (Vapnik 1998; Schlesinger and Hlavac 2002; Heijden et al. 2004; Duda et al. 2001; Webb 2002; Friedman et al. 2000; Jain et al. 2000). It allowed us to recognize arousal from neutral sessions of the experimental protocol. More specifically, results were calculated after twenty steps of cross validation, in particular the training set was composed of 80 % of the whole dataset randomly picked out.

5.2.1 The multi-layer perceptron (MLP)

The Multi-Layer Perceptron (MLP) (KinneBrock 1992) is an artificial neural network model consisting of multiple

layers of nodes mapping sets of input data onto a set of appropriate outputs. Except for the input nodes, each node is a neuron with a nonlinear activation function. This type of network was trained with the help of a supervised learning method, i.e. input and output values were specified and the relations between them learnt. The neural network approximated every non-linear mapping of the form $y = f(x)$. Every data record consisted of input data and the corresponding output data. The multilayer perceptron learnt the input/output behavior of the system examined via a training data set. In the training phase, for each data record, each activation function of the artificial neurons was calculated. The weight w_{ij} of a generic neuron i at the time T , for the input vector $\vec{f}_n^k = f_{n1}^k, \dots, f_{nF}^k$ was modified on the basis of a well established technique, the propagation of the resulting error between the input and the output values. The response of the MLP is a boolean vector; each element represents the activation function of an output neuron. After the training process, the performance of the classification task was evaluated using the confusion matrix. The generic element r_{ij} of the confusion matrix indicates how many times in percentage a pattern belonging to the class i was classified as belonging to the class j . A more diagonal confusion matrix corresponds to a higher degree of classification. As each pattern may be confused with more than one pattern, the sum on each row and column may differ from the value of 100 %. In order to check the generalization capability of the neural network, a cross-validation process is carried out.

6 Experimental results

The International Affective Picture System includes a set of static images based on a dimensional model of emotion. Here we have chosen two classes of images. The first image set included neutral images, such as rolling pin, spoon, mug, trashcan, while the second one contained various pictures depicting mutilations, attack scenes, accidents, i.e. high arousal and negative valence. By way of illustration we report in Fig. 6 an example of neutral image also showing the eye gaze pattern. We do not report intentionally any negatively valenced images because of high visual impact. In Fig. 7 a 3D representation of the eye gaze points over a neutral image is reported. The z-axis represents how many times each pixel was fixated during the presentation time of 10 s. On each image we reported the gaze points. Already at glance, most of neutral images showed a more sparse spatial distribution of the gaze points than the images with arousal, in which gaze points were mainly concentrated into confined areas. A more quantitative analysis was done extracting the above described features from the distribution of eye gaze patterns and

Fig. 6 Example of the points of gaze detected during a neutral elicitation. Gaze points are marked up in red (color figure online)

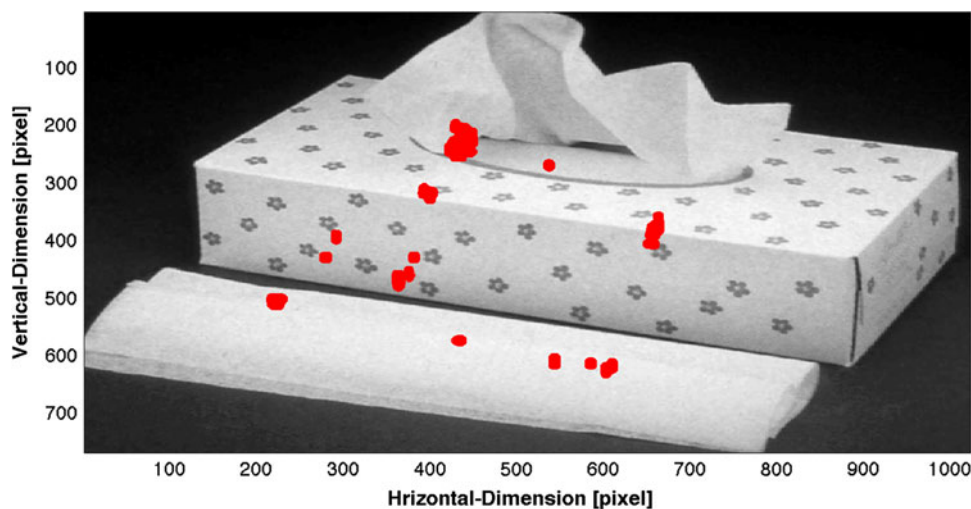


Fig. 7 3D Representation of the gaze points over the image across the recurrence times each pixel was fixated

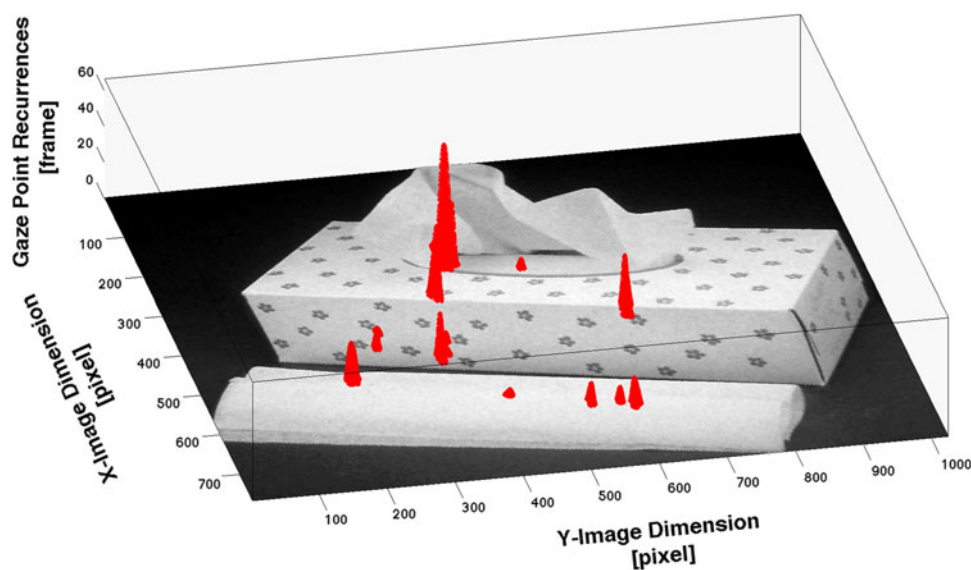


Table 1 Median and deviation of all the extracted features during the visualization of neutral and arousal pictures

Features	Neutral	Arousal
RR*	0.0018 ± 0.0002	0.0019 ± 0.0002
DET**	0.7311 ± 0.0782	0.6373 ± 0.0798
TT**	2.5862 ± 0.9024	2.0345 ± 0.4368
L**	2.9184 ± 0.4564	2.6513 ± 0.3181
ENTR**	1.2592 ± 0.2306	1.0501 ± 0.2041
L _{max} **	5.0000 ± 1.2800	5.0000 ± 1.0583
T _{max} **	1.9600 ± 0.3509	1.5600 ± 0.3501
Pupil	195.39 ± 19.689	197.27 ± 17.106
LGP**	480.0000 ± 208.5236	331.5000 ± 174.1567
MVA**	33.0000 ± 8.8630	27.0000 ± 7.8800

using them as input of the MLP classifier. All the extracted features were not normally distributed, as confirmed by the Lilliefors test, (Lilliefors 1967), which returns a *p-value* ($p < 0.05$) rejecting the null hypothesis of normality. Accordingly, we used the Kruskal-Wallis test, (Kruskal and Wallis 1952), which is a non parametric one-way analysis of variance by ranks for testing equality of population medians. Kruskal-Wallis was performed on ranked data, so the measurement observations were converted to their ranks in the overall data set. This test did assume an identically-shaped and scaled distribution for each group, except for any difference in medians. The null hypothesis was stated as the probability that the samples come from identical populations, regardless their distributions. In place of the mean of distributions we considered the

Table 2 Confusion Matrix of MLP classifier by using the whole set of features

	Neutral	Arousal
Neutral	93.9394 ± 4.2855	20.4545 ± 3.2141
Arousal	6.0606 ± 4.2855	79.5455 ± 3.2141

Bold values represent the correct recognition percentage of the classifier for each specific class

median as measure of location (Stavig and Gibbons 1977). Having only two sets of features, i.e. neutral and arousal classes, Kruskal-Wallis test returned the probability that the two samples were not belonging to the same population, in other words, if there was a statistical difference between the two samples. Median and Median absolute deviation of all the features are reported in Table 1 during the neutral and arousal session. Statistical differences between neutral and arousal elicitation was found (* $p < 0.01$ and ** $p < 0.001$), except for the pupil area detection. We decided however to include this feature in the classification stage, because we verified that the successful recognition percentages increased when using it. Several classifiers, indeed, are not based on statistical rules in the cluster analysis. In the Table 2, the confusion matrix obtained from MLP classifier after twenty fold-cross-validation steps is shown.

7 Conclusions

In this work we investigated eye tracking and pupil size variation in response to emotional elicitation induced by IAPS images. In particular, the goal was to identify a set of features from pupil size variation and eye tracking in order to distinguish between neutral and arousal states. In detail, we used a wearable and wireless head-mounted eye tracking system (HATCAM) to acquire pupil variation together with eye-gaze trajectory as well as time of fixation. In addition, we adopted a novel methodology to characterize differences between neutral and arousal elicitation in eye-gaze acquisitions by means of features extracted from eye gaze patterns using RQA along with specific features extracted from eye gaze trajectory and time of fixation. This choice of RQA, although not specific for this field of application, is motivated by the analogy between the bi-dimensional image containing eye-gaze points and the matrix commonly used for Recurrence Plot (Marwan et al. 2007). Moreover, it resulted to be an effective way to investigate how eye gaze points are geometrically distributed over the the image. More specifically, Recurrence Rate (*RR*) takes into account the density of the gaze points in the images, while Determinism (*DET*), Trapping Time (*TT*), Longest diagonal line (L_{max}) and Entropy (*ENTR*) can show possible and hidden geometrical

distributions of the gaze points. It is worthwhile noting that some specific features, such as *DET*, *TT*, and L_{max} , which are related to some preferred lines, i.e. vertical or diagonal, although apparently not significant, could give relevant geometrical cues in the exploration strategy of the image and, as a matter of fact, increase the successful recognition rate of the classifiers. Our work relies on the conjecture that density and distribution of the eye gaze points on the image are strictly related to the affective content regardless of how graphically the subject is depicted in the image. In this view, we used images whose subject was highly variable in terms of dimensions and form, bot across neutral and arousal sets of pictures. This hypothesis was experimentally confirmed by the significant statistical results reported in Table 1. We tested several classifiers and the best results have been provided by the MLP classifier. After the MLP training process, the performance of the classification task was evaluated by using the confusion matrix. It was randomized for 20-fold cross-validation steps to avoid bias. Results are reported in Table 2. The percentage of successful recognition is higher than 90 % for neutral images and about 80 % for images at high arousal. As it can be seen, results are very satisfactory and improving our previous work (Lanata et al. 2011). It means that eye gaze, both in terms of pupil tracking and size, can be a viable means to discriminate affective states with different arousal content. In that work we used the non parametric K-Nearest Neighbor (K-NN) classifier that was based on the “proximity” concept, i.e. an object was supposed to belong to the closest class. The difference in performance between K-NN and the MLP classifiers can be found in the nature and size of the dataset and it is reduced as the size is increased. In this study the results provided by the MLP improved the previous work, moreover, MLP does not require any previous assumption on the data and being a nonlinear model, it can be applied to model real-world complex relationships (Zhang 2000).

8 Discussions

Since the extracted eye information is regulated by the autonomic nervous system, the results of this experiment suggest that the autonomic nervous system responds differently to emotionally arousing than to emotionally neutral stimuli. Our results are in line with the our recent study (Valenza et al. 2011), that showed changes in the autonomic activity in terms of skin conductance responses, respiration and heart rate variability behavior, during exposition to IAPS images with different arousal content. Even though our results showed a significant information from eye gaze pattern, however, they did not show significant pupil size differences among IAPS stimulation. In

the literature there are discordant works about the pupil size variation upon affective stimuli. In the study of Loewenfeld (1966) it is reported that pupil size may not be sensitive enough to discriminate emotional responses, while Hess (1972) and Partala and Surakka (2003) showed experimental evidence about this affective-dependence variation. In our study, pupil size does not seem to have a relevant role, but it could also be explained in terms of low resolution of the camera used in the HATCAM system, which did not detect the fine pupil responses, or of a possible failure in providing right controlled stimuli, considering also that there are several factors affecting the variation of pupil size. Hess and Petrovich (1987) listed several different sources of pupil size variation, including, for example, the light reflex, different stimulus parameters (e.g. visual and chemical), and information-processing load. However, besides the role of pupil size, our results are very satisfactory and very promising for the use of eye information pattern in the context of pervasive monitoring. This would extend the perceptually intelligent abilities of an engine to perceive and analyze human behavior. In human behavior positive emotions have been argued to increase creativity, to help in creating richer associations for memorized material, and to realize more efficient decision-making machines (Isen and Means 1983; Zhou 1998). In addition, by using suitable emotion-related cues, it could be also possible to modulate the user emotional reactions that could be used also as possible therapy in mental disease management. Future work will progress to exploit eye gaze together with peripheral physiological signals in the field of human behavior understanding and mental care.

Acknowledgments This research is partially supported by the EU Commission under contract FP7-ICT-247777 Psyche, and partially supported by the EU Commission under contract FP7-ICT-258749 CEEDs.

References

- Andreassi JL (2006) Psychophysiology Human behavior and physiological response. Lawrence Erlbaum Assoc Inc., ISBN: 0805849513
- Armato A, Lanatà A, Scilingo EP (2011) Comparative study on photometric normalization algorithms for an innovative, robust and real-time eye gaze tracker. *J Real-Time Image Process* 1–13. doi:10.1007/s11554-011-0217-6
- ASL (2009) Applied science laboratories: mobile eye and eye tracking services. <http://www.asleyetracking.com>
- Beatty J, Lucero-Wagoner B (2000) The pupillary system. Cambridge University Press, Cambridge
- Bennett N, Burrige R, Saito N (2002) A method to detect and characterize ellipses using the Hough transform. *IEEE Trans Pattern Anal Mach Intell* 21(7):652–657
- Bradley MM, Sabatinelli D, Lang PJ, Fitzsimmons JR, King W, Desai P (2003) Activation of the visual cortex in motivated attention. *Behav Neurosci* 117(2):369
- Calvo MG, Lang PJ (2004) Gaze patterns when looking at emotional pictures: motivationally biased attention. *Motiv Emot* 28(3):221–243
- Chen W, Er MJ, Wu S (2006) Illumination compensation and normalization for robust face recognition using discrete cosine transform in logarithm domain. *IEEE Trans Syst Man Cybernet Part B Cybernet* 36(2):458–466
- Christianson SÅ, Loftus EF, Hoffman H, Loftus GR (1991) Eye fixations and memory for emotional events. *J Exp Psychol Learn Memory Cognit* 17(4):693
- Damasio AR (2000) *Descartes' error: emotion, reason, and the human brain*. Quill, New York, ISBN: 0380726475
- Darwin C, Ekman P, Prodger P (2002) *The expression of the emotions in man and animals*. Oxford University Press, Oxford, ISBN: 0195158067
- Duda R, Hart P, Stork D (2001) *Pattern classification*, 2nd edn. Wiley, New York
- Ekman P, Levenson RW, Friesen WV (1983) Autonomic nervous system activity distinguishes among emotions. *Science*, ISSN: 0036-8075
- Fitzgibbon A, Pilu M, Fisher RB (2002) Direct least square fitting of ellipses. *IEEE Trans Pattern Anal Mach Intell* 21(5):476–480
- Forsyth DA, Ponce J (2002) *Computer vision: a modern approach*, Professional Technical Reference. Prentice Hall, Upper Saddle River
- Friedman J, Hastie T, Tibshirani R (2000) Additive logistic regression: A statistical view of boosting. *Annals Stat* 38(2):337–374
- Gross JJ, Muñoz RF (1995) Emotion regulation and mental health. *Clin Psychol Sci Pract* 2(2):151–164
- Heijden F, Duin R, Ridder D, Tax D (2004) *Classification, parameter estimation and state estimation*. Wiley, New York
- Hess EH (1972) Pupillometrics: a method of studying mental, emotional and sensory processes, handbook of psychophysiology. Holt, Rinehart & Winston, New York, pp 91–531
- Hess EH, Petrovich SB (1987) Pupillary behavior in communication: nonverbal behaviour and communication. Erlbaum, Hillsdale, pp 327–348
- ISCAN (2007) Inc. Eye and target tracking solutions. <http://www.iscaninc.com/>
- Isen AM, Means B (1983) The influence of positive affect on decision-making strategy. *Soc Cognit* 2(1):18–31
- Jain AK, Duin RPW, Mao J (2000) Statistical pattern recognition: a review. *IEEE Trans Pattern Anal Mach Intell* 22(1):4–37
- Janisse MP (1974) Pupil size, affect and exposure frequency. *Soc Behav Pers* 2(2):125–146
- KinneBrock W (1992) *Neural networks*. Oldenburg Verlag, Munchen
- Kruskal WH, Wallis WA (1952) Use of ranks in one-criterion variance analysis. *J Am Stat Assoc* 47(260):583–621
- Lanatà A, Armato A, Valenza G, Scilingo EP (2011) Eye tracking and pupil size variation as response to affective stimuli: a preliminary study. In: 2011 5th international conference on pervasive computing technologies for healthcare (pervasive health), IEEE, pp 78–84
- Land EH, McCann JJ (1971) Lightness and retinex theory. *J Opt Soc Am* 61(1):1–11
- Lang PJ, Bradley MM, Cuthbert BN (1997) International affective picture system (IAPS): Technical manual and affective ratings. NIMH Center for the Study of Emotion and Attention
- Lazarus RS, Averill JR (1972) Emotion and cognition: With special reference to anxiety. *Anxiety Curr Trends Theory Res* 2:242–284
- Levenson RW (1992) Autonomic nervous system differences among emotions. *Psychol Sci* 3(1):23
- Li D, Babcock J, Parkhurst DJ (2006) openeyes: a low-cost head-mounted eye-tracking solution. In: *Proceedings of the 2006*

- symposium on Eye tracking research and applications, ACM, pp 95–100
- Lilliefors HW (1967) On the Kolmogorov-Smirnov test for normality with mean and variance unknown. *J Am Stat Assoc* 62(318):399–402
- Loewenfeld IE (1966) Comment on hess' findings. *Surv Ophthalmol* 11:293–294
- Lohse GL, Johnson EJ (2002) A comparison of two process tracing methods for choice tasks. In: *Proceedings of the Twenty-Ninth Hawaii International Conference on System sciences, 1996*, vol 4, pp 86–97. IEEE, ISBN 0818673249
- Maini E (2005) Robust ellipse-specific fitting for real-time machine vision. In: *Brain, vision, and artificial intelligence*. Springer, Berlin, pp 318–327
- Marwan N, Carmen Romano M, Thiel M, Kurths J (2007) Recurrence plots for the analysis of complex systems. *Phys Reports* 438(5–6):237–329
- Partala T, Surakka V (2003) Pupil size variation as an indication of affective processing. *Int J Human-Comput Stud* 59(1):185–198
- Picard RW (2000) *Affective computing*. The MIT Press, Cambridge, ISBN 0262661152
- Schlesinger M, Hlavac V (2002) *Ten lectures on statistical and structural pattern recognition*. Kluwer Academic Publishers, Dordrecht
- SMI (2011) *Sensomotoric instruments: gaze and eye tracking systems*. <http://www.smivision.com/>
- S R Research Ltd. (2010) *S R research:complete eye tracking solutions*. <http://www.sr-research.com/>
- Stavig GR, Gibbons JD (1977) Comparing the mean and the median as measures of centrality. *Int Stat Rev/Revue Internationale de Statistique* 45(1):63–70
- TOBII Technology (2011) *Tobii eye tracking innovator*. <http://www.tobii.com/>
- Valenza G, LanatàA, Scilingo E (2011) The role of nonlinear dynamics in affective valence and arousal recognition. *EEE Trans Affect Comput*. doi:10.1109/T-AFFC.2011.30
- Vapnik V (1998) *Statistical learning theory*. Wiley, New York
- Webb A (2002) *Statistical pattern recognition*. Wiley, New York
- Zajonc RB (1984) On the primacy of affect. *Am Psychol* 39(2):117–123
- Zbilut JP, Webber Jr CL (1994) *Recurrence quantification analysis*. Wiley Online Library
- Zhang GP (2000) Neural networks for classification: a survey. *IEEE Trans Syst Man Cybernet Part C Appl Rev* 30(4):451–462
- Zhou J (1998) Feedback svalence, feedback style, task autonomy, and achievement orientation: interactive effects on creative performance. *J Appl Psychol* 83(2):261